

# Modifications in the chemical structure of Trojan carriers: impact on cargo delivery†

Baptiste Aussedat,<sup>\*a</sup> Edmond Dupont,<sup>b</sup> Sandrine Sagan,<sup>a</sup> Alain Joliot,<sup>b</sup> Solange Lavielle,<sup>a</sup> Gérard Chassaing<sup>a</sup> and Fabienne Burlina<sup>\*a</sup>

Received (in Cambridge, UK) 10th January 2008, Accepted 7th February 2008

First published as an Advance Article on the web 22nd February 2008

DOI: 10.1039/b800433a

**Carriers with linear or dendrimeric structures displaying different functional groups were synthesized and their delivery properties were studied.**

Cellular delivery of biopolymers remains an important problem of cell biology and medicine. Trojan peptides or cell-penetrating peptides (CPPs) are promising tools for delivering bioactive cargoes which are poorly internalized by themselves such as oligonucleotides, peptides and proteins.<sup>1</sup> One of the challenges now is to design CPPs with improved efficiencies of delivery and which can specifically target cargoes to the different cellular organelles. In this context, we have studied the impact on cargo delivery of modifications in the CPP chemical structure. For this, we have designed a small library of pseudo-peptide carriers displaying different functional groups which are known to promote CPP cellular uptake (ammonium or guanidinium<sup>2</sup> and myristyl<sup>3</sup>). Carriers were synthesized by modular assembly from the 'bis-ornithine' scaffold<sup>4</sup> to give linear or dendrimeric structures and allow different spatial arrangements of the functional groups (Fig. 1). The classical CPPs Lys<sub>9</sub>, Arg<sub>9</sub>,<sup>2</sup> Penetratin (Pen)<sup>5</sup> and Kno<sup>6</sup> were used as references (see ESI† for sequences).

The cargo that was chosen is a hydrophilic peptide corresponding to the protein kinase C- $\alpha/\beta$  pseudo-substrate (PKCi, Fig. 1),<sup>7</sup> which is poorly internalized by itself into cells.<sup>5,6</sup> The PKCi peptide was linked to the carriers *via* a disulfide bond, which should be reduced in some compartments of the cell leading to the release of the cargo.<sup>8</sup> Our approach has consisted of tracking the internalized cargo using a method based on MALDI-TOF mass spectrometry (MS).<sup>6,9</sup> This directly gives the amount of intact intracellular cargo and also allows the characterization of the fragments produced by intracellular proteases. The comparison of the digestion profiles of the same cargo delivered by different carriers can give relevant information for the problem addressed here since degradation is related to the cargo trafficking and/or final localization. Concomitantly, the cargo distribution in cells was examined by confocal microscopy.

The pseudo-peptide carriers were obtained by modular construction from the  $\alpha,\alpha$ -disubstituted amino acid 'bis-ornithine' (Fig. 1). To overcome the low reactivity of the 'bis-ornithine' resulting from the steric hindrance of the  $\alpha$ -nitrogen and ensure efficient solid phase polymer assembly, we have synthesized in solution dipeptide units containing a spacer ( $\beta$ Ala or Gly) as described before.<sup>4</sup> The *N*-terminal and side chain amines were protected uniformly or orthogonally yielding a great versatility in the design of polymers: (i) linear polymer by stepwise elongation from the *N*-terminus (carriers L1 to L5), (ii) branched polymer by differential elongation from the *N*-terminus and side chains (B1) and (iii) homo- or hetero-functionalized dendrimers by parallel elongation from all amines (D1 and D2) (Fig. 1). High coupling yields were obtained using PyAOP–HOAt activation. Carriers were conjugated in solution to the PKCi cargo (see ESI†).

The amount of intact PKCi transported into CHO cells by the different carriers was measured by MALDI-TOF MS as described previously (see results in Fig. 2 and in ESI†).<sup>6</sup> The cargo is biotinylated to allow an easy recovery (performed in reducing conditions, see ESI†), concentration and desalting before MS analysis. Quantification is based on the use of an internal standard corresponding to the free cargo labeled by deuterium (Fig. 1). The CPP Arg<sub>9</sub> was found to be more efficient than Lys<sub>9</sub> in transporting the PKCi cargo, in agreement with previous data.<sup>2</sup> However, no difference was observed between carriers L1 and L2 containing four 'bis-ornithine' and 'bis-arginine' residues, respectively. It has been shown before that increasing the backbone flexibility of poly-guanidine transporters improves their cellular uptake probably by allowing a better interaction of the cationic groups with negatively charged membrane components.<sup>10</sup> The side chains of the 'bis-ornithine' residues were elongated (L3) to increase the potential surface of interaction of the guanidiniums with the membrane. Alternatively, a dendrimeric backbone was used (D1) to obtain a more globular display of the guanidinium groups. These modifications had no impact on the efficiency of cargo delivery. In contrast, myristoylation significantly enhanced the efficiency of delivery in the pseudo-peptide series (7-fold between L2 and L4). Interestingly, the efficiency was unaltered when reducing the number of 'bis-arginine' residues from four (in L4) to one to give the minimalist carrier L5. Increasing the number of myristyl groups of the carrier (D2) had no significant effect. We then designed compound B1 by combining the structure of the efficient myristoylated carrier L4 with a branched domain to

<sup>a</sup> UPMC Univ. Paris 06, CNRS UMR 7613, 4 place Jussieu, F-75005 Paris, France. E-mail: bausseadat@gmail.com. E-mail: burlina@ccr.jussieu.fr; Fax: +33 (0)144273843; Tel: +33 (0)144273115

<sup>b</sup> Ecole Normale Supérieure, CNRS UMR 8542, 46 rue d'Ulm, 75005 Paris, France

† Electronic supplementary information (ESI) available: Protocols for compound synthesis and study. See DOI: 10.1039/b800433a

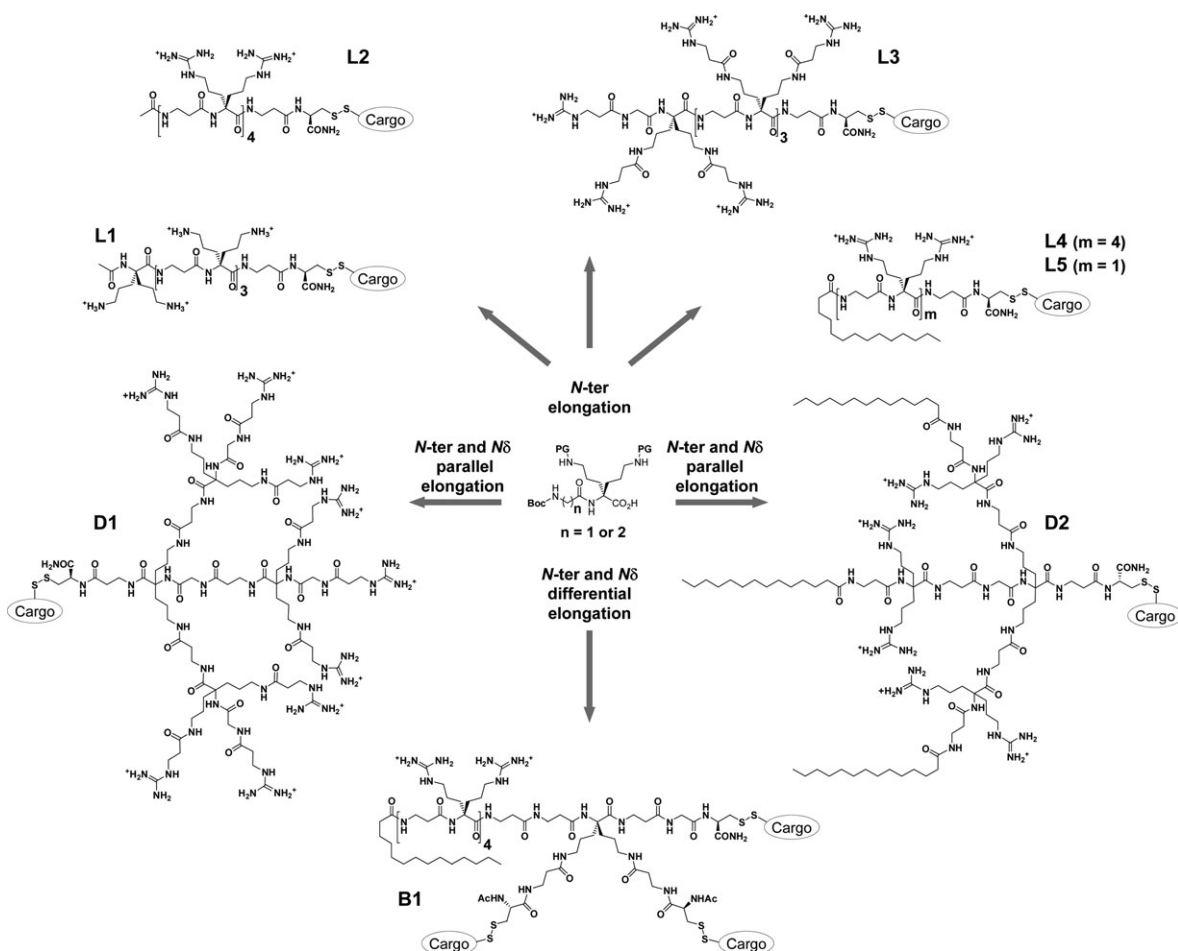


**Fig. 1** Structures of the carrier–cargo conjugates and dipeptide units derived from ‘bis-ornithine’. *N*-ter and *N*δ designate the *N*-terminal and side chain amines, respectively, PG corresponds to Boc or Alloc protecting group. The PKCi cargo (CRFARKGALRQKNV) contains on its *N*-terminus a biotin-GGGG isotope-labeling/affinity tag for MS quantification (non deuterated G for the internalized conjugates, deuterated G for the internal standard).

attach three cargoes. With this construction, the amount of internalized cargo could be further increased. Indeed, the B1–(PKCi)<sub>3</sub> conjugate led to an intracellular concentration of PKCi ( $46.2 \pm 2.2 \mu\text{M}$ , see ESI†) three times higher than the one obtained with L4–PKCi ( $14.5 \pm 1.4 \mu\text{M}$ ) using the same extracellular concentration of conjugate ( $7.5 \mu\text{M}$ ). These data are interesting also because they show that carrier L4 is internalized with the same efficiency when linked to one or three cargo molecules despite the structural changes between

the resulting conjugates. Finally, some classical CPPs were also myristoylated for comparison (see results in Fig. S1 of the ESI†). Myristoylation notably improved the efficiency of Arg<sub>9</sub> (5-fold) as previously reported for this CPP<sup>3</sup> and other peptides<sup>11–13</sup> but it had little effect in the case of Kno and Pen. The effect of myristoylation on cellular uptake is thus highly dependent on the peptide sequence.

The profile of degradation of the PKCi cargo was then compared depending on the pseudo-peptide carrier used (Fig. 3 and Figs. S3 and S4 in the ESI†). For this, the relative abundances of the ions corresponding to the intact cargo and the biotinylated digests were calculated from the mass spectra of the internalization experiments. The intact cargo was in all cases the most abundantly detected species. Cleavage on the *C*-terminus of basic residues of PKCi was observed with all carriers. Interestingly, cleavage after one or both Ala residues of PKCi was observed only when it was delivered by myristoylated carriers (all except L5). These data thus reveal differences in the trafficking or distribution of the internalized cargo depending on the nature of the transporter.

The intracellular localization of the PKCi cargo was then examined by confocal microscopy. Because the properties of

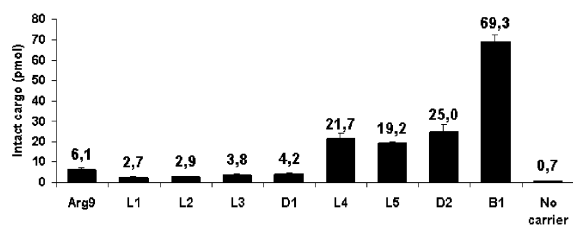


**Fig. 2** Total amount of intact cargo in  $10^6$  CHO cells determined by MALDI-TOF MS. Cells were incubated with the conjugates ( $7.5 \mu\text{M}$ ) for 75 min at  $37^\circ\text{C}$ . Each of the data is the average result of three independent experiments performed in duplicate  $\pm$  SEM.

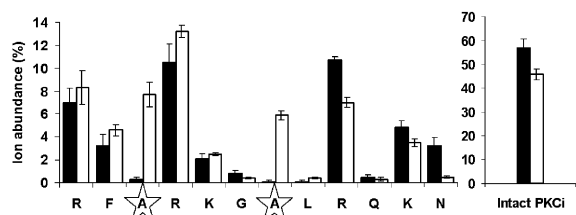


**Fig. 3** Degradation profile of the PKCi cargo when transported by L2 (black bars) and L4 (white bars) determined by MALDI-TOF MS. Relative ion abundance was calculated from the signal areas (average  $\pm$  SEM). The C-terminal residue of the digests is indicated. Only biotinylated species are recovered and may be detected (see ESI<sup>†</sup>).

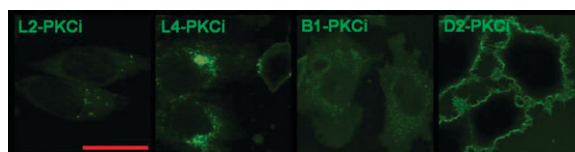


**Fig. 4** Confocal microscopy images showing the intracellular distribution of the cargo when delivered by different carriers. CHO cells were incubated with the conjugate (10  $\mu$ M) for 30 min at 37  $^{\circ}$ C. Biotinylated cargo was revealed by Alexa-488-streptavidin. The scale bar represents 20  $\mu$ m.

some CPPs are altered upon carboxyfluorescein functionalization<sup>14</sup> and because organic fixation could induce the artefactual redistribution of CPPs,<sup>15</sup> the internalized biotinylated PKCi was revealed as described previously.<sup>14</sup> Briefly, the extracellular peptide was quenched with unlabeled streptavidin and following fixation with paraformaldehyde and membrane permeabilization, the intracellular peptide was revealed with fluorescent streptavidin. The intracellular distribution of the cargo varied strongly with the carrier used (see Figs. 4 and S5 in the ESI<sup>†</sup>). With all the non-myristoylated pseudo-peptide carriers, a faint fluorescence signal was detected mainly in endosomes. Myristoylated carriers gave different cargo localizations. With L4 and L5 the staining was mostly found in perinuclear vesicular structures and was visible throughout the cytosol. This diffuse cytosolic fluorescence was further enhanced with B1, together with the detection of some nuclear staining. Finally with D2, the staining was restricted to the vicinity of the plasma membrane. The three myristyl groups of D2 appear to anchor the conjugate to the membrane. The biotin moiety of the cargo is accessible to streptavidin only after membrane permeabilization, suggesting that it faces the cytoplasm or is embedded in the membrane. However, the disulfide bridge between the carrier and cargo is not accessible to the cytosolic glutathione since no cargo is visualized in the cytosol. When assessed with Arg<sub>9</sub> carriers, the predominant

nuclear accumulation obtained with the Arg<sub>9</sub>-PKCi conjugate was strongly shifted toward the cytosol upon myristoylation (ESI<sup>†</sup>).

In conclusion, we have shown here the great versatility of the 'bis-ornithine' scaffold for the solid phase synthesis of polymers with linear, branched or dendrimeric structures and bearing different functional groups. Changing the nature or spatial arrangement of the cationic groups of the carrier had little effect on the efficiency of cargo delivery. Cellular uptake was improved by myristoylation. Interestingly, it was found that the myristoylated carrier L4 was able to transport several cargoes at the same time, allowing an increase of the cargo intracellular amount. Our data also provide evidence that distinctive intracellular localizations and degradation of the cargo can be obtained by changing the chemical structure of the carrier. Work is in progress to identify the organelle(s) that can be accessed with some of these new carriers.

We would like to thank Prof. A. Prochiantz and Dr G. Bolbach for fruitful discussions. We are very grateful to G. Clodic for recording the mass spectra. We thank for financial support the ANR (Prob-DOM), the EC (Nano4drugs, contract LSHC-CT-2005-019102) and the MENRT and Fondation pour la Recherche Médicale (PhD fellowship for B. A.).

## Notes and references

- G. P. Dietz and M. Bahr, *Mol. Cell. Neurosci.*, 2004, **27**, 85–131.
- D. J. Mitchell, D. T. Kim, L. Steinman, C. G. Fathman and J. B. Rothbard, *J. Pept. Res.*, 2000, **56**, 318–325.
- W. Pham, M. F. Kircher, R. Weissleder and C. H. Tung, *ChemBioChem*, 2004, **5**, 1148–1151.
- B. Aussedat, G. Chassaing, S. Lavielle and F. Burlina, *Tetrahedron Lett.*, 2006, **47**, 3723–3726.
- L. Theodore, D. Derossi, G. Chassaing, B. Llibat, M. Kubes, P. Jordan, H. Chneiweiss, P. Godement and A. Prochiantz, *J. Neurosci.*, 1995, **15**, 7158–7167.
- B. Aussedat, S. Sagan, G. Chassaing, G. Bolbach and F. Burlina, *Biochim. Biophys. Acta*, 2006, **1758**, 375–383.
- C. House and B. E. Kemp, *Science*, 1987, **238**, 1726–1728.
- G. Saito, J. A. Swanson and K. D. Lee, *Adv. Drug Delivery Rev.*, 2003, **55**, 199–215.
- F. Burlina, S. Sagan, G. Bolbach and G. Chassaing, *Angew. Chem., Int. Ed.*, 2005, **44**, 4244–4247.
- J. B. Rothbard, E. Kreider, C. L. VanDeusen, L. Wright, B. L. Wylie and P. A. Wender, *J. Med. Chem.*, 2002, **45**, 3612–3618.
- T. Eichholtz, D. B. de Bont, J. de Widt, R. M. Liskamp and H. L. Ploegh, *J. Biol. Chem.*, 1993, **268**, 1982–1986.
- H. M. Ekrami, A. R. Kennedy and W. C. Shen, *FEBS Lett.*, 1995, **371**, 283–286.
- A. R. Nelson, L. Borland, N. L. Allbritton and C. E. Sims, *Biochemistry*, 2007, **46**, 14771–14781.
- E. Dupont, A. Prochiantz and A. Joliot, *J. Biol. Chem.*, 2007, **282**, 8994–9000.
- J. P. Richard, K. Melikov, E. Vives, C. Ramos, B. Verbeure, M. J. Gait, L. V. Chernomordik and B. Lebleu, *J. Biol. Chem.*, 2003, **278**, 585–590.